ChemComm

COMMUNICATION

View Article Online
View Journal | View Issue

Cite this: *Chem. Commun.*, 2016, 52, 9387

Received 8th June 2016,
Accepted 23rd June 2016

DOI: 10.1039/c6cc04786f

www.rsc.org/chemcomm

Dynamic nanoproteins: self-assembled peptide surfaces on monolayer protected gold nanoparticles†

Sergio Garcia Martin and Leonard J. Prins*

Here, we demonstrate the formation of dynamic peptide surfaces through the self-assembly of small peptides on the surface of monolayer protected gold nanoparticles. The complexity of the peptide surface can be simply tuned by changing the chemical nature of the added peptides and the ratio in which these are added. The dynamic nature of the surface permits adaptation to changes in the environment.

The exquisite properties of proteins in terms of molecular recognition and catalysis derive in large part from their size and structural complexity.[1] Their size permits the presence of internal cavities, which are well-shielded from the bulk solvent[2] and permit additional advantages like allosteric control by secondary binding sites[3] and multivalent interactions to drive protein–protein interactions.[4] The fact that all proteins are composed of a very limited number of amino acids renders these structures even more fascinating. Currently, a strong impetus exists to develop synthetic structures able to match the size and complexity of proteins for applications in diagnostics, medicine and materials science.[5,6] The advantage of synthetic structures is the ability to design the desired structure and the possibility of including also non-natural building blocks. Generally, the followed approach relies on the decoration of multivalent scaffolds, such as polymers[7] or nanoparticles,[8] with amino acids or small peptides, although the self-assembly of small (peptidic) molecules has also been extensively used.[9] Here, we exploit a combination of both approaches for the formation of multivalent peptide surfaces on monolayer protected gold nanoparticles. In the last few years we have extensively used Au NP **1**, which are gold nanoparticles (d = 1.8 ± 0.4 nm) covered with a monolayer of C9-thiols terminating with a 1,4,7-triazacyclonane (TACN)·Zn^{2+} head group, for applications in sensing, catalysis, and systems chemistry.[10] A majority of these applications rely on the high affinity of small oligoanions, such as peptides and nucleotides, for the highly positively charged surface of Au NP **1**. Binding constants were high enough to ensure binding of multiple molecules under saturation conditions even at low micromolar concentrations under physiologically relevant conditions. Yet, the noncovalent interactions that drive the self-assembly processes ensure that spontaneous exchange processes occur on the monolayer surface. Here, we show that these two features create the possibility of forming multivalent peptide surfaces simply by assembling multiple small peptide sequences on Au NP **1**. It will be shown that such an approach offers several advantages. The self-assembly process facilitates the formation of nanoproteins, since just mixing the components under ambient conditions is sufficient. The complexity of the multivalent surface can not only be simply tuned by changing the peptide sequence, but also by changing the ratio of the added peptides. Finally, the dynamic nature of the peptide surface implies that spontaneous adaptation of the surface is possible, enabling the possibility of exploiting dynamic combinatorial chemistry on nanoparticle surfaces.[11–13]

A series of seven different pentapeptides (**I–VII**) with the general sequence Ac-XXGWS(OPO_3^{2-})-OH was prepared (Fig. 1). The constant domain was composed of a phosphorylated Ser-residue for binding to Au NP **1**, a fluorescent Trp-residue for monitoring the binding interaction and a Gly-residue as a flexible spacer to outdistance the two remaining residues of the variable domain. The residues of the variable domain X were chosen from the various subgroups of amino acids ranging from apolar (Phe (**I**), Leu (**II**)), polar neutral (Asn (**III**), Ser (**IV**)), anionic (Asp (**V**)), to cationic (Lys (**VI**), Arg (**VII**)) in order to explore the compatibility with the self-assembly process (Fig. 1). Two residues of each amino acid were added to enhance their contribution to the overall properties of the corresponding peptide. Fluorescence titration experiments of the peptides at a fixed concentration of Au NP **1** ([TACN·Zn^{2+}] = 10 μM) in aqueous buffer at pH = 7.0 revealed a high affinity of all peptides, except for **VI** and **VII** (Fig. 2a). The shallow curvature of the binding isotherms of the latter peptides, as compared to those of peptides **I–V**, indicates that these peptides bind Au NP

Department of Chemical Sciences, University of Padova, Via Marzolo 1, 35131 Padova, Italy. E-mail: leonard.prins@unipd.it; Fax: +39 049 8275051

† Electronic supplementary information (ESI) available: Experimental details and control experiments. See DOI: 10.1039/c6cc04786f

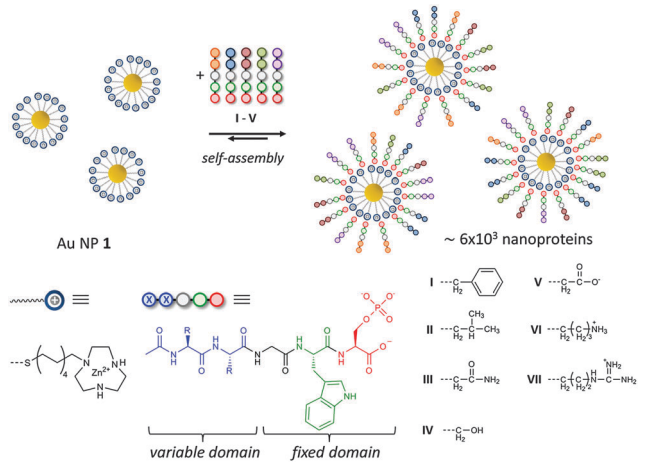

Fig. 1 Schematic representation of the self-assembly of dynamic nanoproteins.

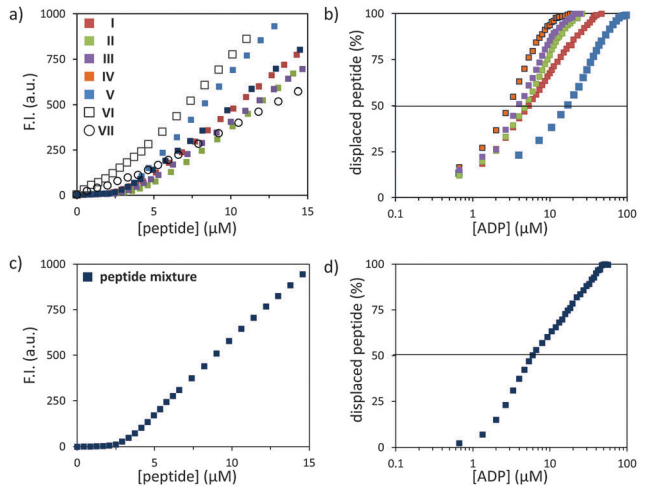

Fig. 2 (a) Fluorescence intensity at 360 nm as a function of the concentration of peptide **I–V** added to Au NP **1**. (b) Amount of displaced peptide **I–V** from the surface of Au NP **1** as a function of the concentration of ADP. (c) Fluorescence intensity at 360 nm as a function of the concentration of a mixture of peptides **I–V** added to Au NP **1**. (d) Amount of displaced peptide mixture from the surface of Au NP **1** as a function of the concentration of ADP. Experimental conditions: [TACN·Zn^{2+}] = 10 ± 1 μM; [HEPES] = 10 mM, pH 7.0.

1 with a much lower affinity. This is tentatively ascribed to the neutralization of the negative charges of the constant domain by the positively charged Lys- and Arg-residues, which cancels the main driving force for binding. For this reason, peptides **VI** and **VII** were discarded from further studies. For other peptides **I–V** surface saturation concentrations (SSCs) ranging from 3.1 to 4.3 μM were determined (Table S2, ESI†). Considering that the monolayer of Au NP **1** with a diameter of 1.8 ± 0.4 nm contains around 70 thiols, this implies that at saturation around 20–30 peptides are bound simultaneously to the monolayer.[14] This indicates that truly multivalent systems are spontaneously formed. The dynamic nature of these systems emerged from competition experiments in which the addition of an increasing amount of adenosine diphosphate (ADP) resulted in the progressive displacement of peptides from Au NP **1**. The ADP-concentration required to displace 50% of peptide was used as a value to assess the relative affinities of peptides **I–V** for Au NP **1** (Table S2, ESI†). Interestingly, whereas all peptides have an intrinsic high affinity for Au NP **1** because of the phosphoSer residue, it turns out that the variable domain caused significant variations. Peptides with apolar residues like Phe (**I**) or Leu (**II**) had higher affinities compared to those with polar residues Asn (**III**) and Ser (**IV**), which is in line with previous studies that hydrophobic interactions also contribute to the interaction between external agents and Au NPs.[15] Not surprisingly, the highest affinity for Au NP **1** was observed for peptide **V**, which has two additional negative charges (Fig. 2b).

Having established the nature of the interactions between the individual peptides and Au NP **1** we then proceeded with the study of systems of higher complexity. An equimolar mixture of peptides **I–V** was prepared and titrated to Au NP **1** ([TACN·Zn^{2+}] = 10 μM) yielding a binding isotherm similar to that observed for the separate binding isotherms, which demonstrates that different peptides can be accommodated simultaneously on Au NP **1** (Fig. 2c). An SSC of 2.4 μM was determined for the peptide mixture indicating that under these conditions the surface of Au NP **1** is saturated with around 17 peptides. This value is lower than that observed for pure peptides, which suggests that packing is less efficient when different peptides co-assemble on the surface. In any case, the high complexity of the self-assembled system emerges from the calculation of the number of different peptide surfaces that are created upon the addition of the peptide mixture. Assuming that all binding sites are identical and independent, the total number of different combinations, C, is given by

$$C = \frac{(N+1)\times(N+2)\times\cdots(N+k-1)}{2\times 3\times\cdots(k-1)} \qquad (1)$$

with N being the number of available (degenerate) binding sites and k being the number of peptides. This implies that the addition of peptides **I–V** (k = 5) to Au NP **1** (N = 17) results in the spontaneous formation of around 6 × 10^3 different peptide surfaces. A displacement experiment using ADP confirmed the dynamic nature of these surfaces. The irregular nature of the displacement curve reflects the different binding affinities of peptides **I–V**: addition of incremental amounts of ADP results first in the displacement of those peptides with lower binding affinities (Fig. 2d).

We then proceeded with a proof-of-principle study aimed at demonstrating the responsive nature of the dynamic peptide surface. However, this first required a methodology to monitor the surface composition and changes therein, since the fluorescence titrations did not provide this kind of information. We found that ultracentrifugation using PES-membranes with a 10 kDa molecular weight (MW) cut-off permitted the facile separation of surface bound peptides from nonbound peptides.[16] LC/MS-analysis of the filtrate gave the concentration of each peptide in solution, from which the surface composition could then be calculated considering that the initial peptide

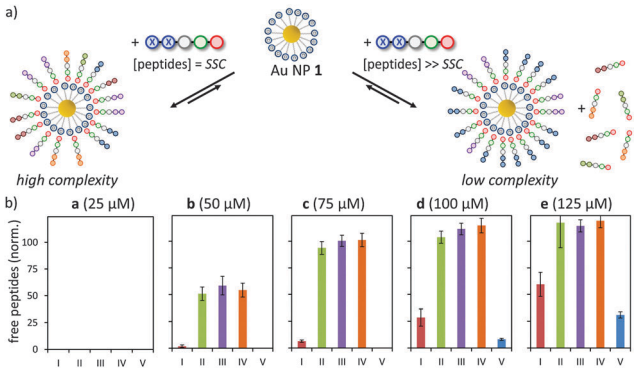

Fig. 3 (a) Schematic representation of the peptide surface complexity as a function of the peptide concentration. SSC refers to the surface saturation concentration. (b) Concentration of peptides **I–V** in the filtrate after centrifugation of peptide mixtures a–e and Au NP **1**. Each peptide concentration was normalized on the intensity of reference peaks obtained from centrifugation of the same samples in the absence of Au NP **1**. Experimental conditions: [TACN·Zn^{2+}] = 50 ± 5 μM; [HEPES] = 10 mM, pH 7.0. Ultrafiltration procedure: PES membrane with 10 kDa MW cut-off, centrifugation at 12 000 rpm for 15 s, starting volume = 500 μl, filtrate volume ~100 μl.

concentrations are known. This protocol was then applied to determine the surface composition of peptides **I–V** on Au NP **1** as a function of the initial peptide concentration. An equimolar mixture of peptides **I–V** was added to Au NP **1** ([TACN·Zn^{2+}] = 50 μM) at five different concentrations a–e (25, 50, 75, 100 and 125 μM – referring to the overall peptide concentrations). Compared to the fluorescence binding studies, a higher concentration of Au NP **1** was necessary to permit detection of the peptides by LC/MS. It is noted that at this higher concentration a significantly higher SSC of 25 μM was determined for the peptide mixture (see Fig. S8, ESI†). After addition, each sample was centrifuged and the filtrate was analyzed by LC/MS in single ion detection mode. For each peptide, the peak area was normalized on the area measured for the same mixture centrifuged in the absence of Au NP **1**. Each experiment was repeated 5 times to give the average values and error margins indicated in Fig. 3.

The absence of peptides in the filtrate of sample a (25 μM) confirms that at this concentration all peptides are bound to Au NP **1**, which is in agreement with the fluorescence studies. This was further confirmed by a control experiment in which an excess of adenosine triphosphate (ATP) was added to sample a before filtration. ATP is a strong competitor and displaces all peptides from the surface leading to an increase in the concentration of peptides in the filtrate (see Fig. S10, ESI†).

At peptide concentrations higher than the SSC (samples b–e) a competition has to necessarily take place between the peptides for binding to the limited number of binding positions on Au NP **1**, thus creating the conditions for observing a spontaneous adaptation of the surface. Indeed, for all these samples the presence of nonbound peptides resulted in their presence in the filtrate (Fig. 3b). Interestingly, a clear differentiation was observed between the peptides as the concentrations increased from 50 to 125 μM. The surface composition became biased towards peptides **I** and **V**, which are indeed those peptides with a higher affinity for Au NP **1**. At the highest concentration of 125 μM the assembled peptide surface is composed of 30% of **I** and 70% of **V**; peptides **II–IV** are no longer present on the surface of Au NP **1**. These experiments demonstrate the ability of the peptide surface to spontaneously adapt to changes in the environment. In this particular case, the result is a shift from a highly complex peptide surface containing all peptides **I–V** in equimolar amounts to a surface dominated by peptides **I** (30%) and **V** (70%).

In conclusion, we have shown that the self-assembly of small peptides on Au NP **1** is an attractive way to create multivalent peptide surfaces. The resulting systems have a size and complexity similar to proteins and are stable at low micromolar concentrations in aqueous buffer. The surface composition can be simply tuned by changing the nature and ratio of the added peptide fragments. The dynamic nature of the surface permits adaptation of the surface to changes in the environment and offers the possibility of developing self-selection protocols. Combined with a covalent fixation methodology, such as the light-triggered immobilization of peptides on gold nanoparticles that we have reported earlier,[17] this approach gives a straightforward access to self-selected multivalent peptide surfaces. We envision that this approach may be used for molecular imprinting of the monolayer to create self-selected active sites for the recognition of small biomolecules or for catalysis, and for the self-selection of peptide surfaces able to interfere with protein–protein interactions.

Financial support from the Marie Curie ITN READ (289723) is acknowledged. We thank Prof. Cinzia Mortarino (Department of Statistical Sciences, University of Padova) for help with the statistical calculations.

References

1 A. Fersht, *Structure and Mechanism of Protein Science*, W. H. Freeman & Company, New York, 1999.
2 E. Persch, O. Dumele and F. Diederich, *Angew. Chem., Int. Ed.*, 2015, **54**, 3290–3327.
3 B. Bukau, J. Weissman and A. Horwich, *Cell*, 2006, **125**, 443–451.
4 J. A. Wells and C. L. McClendon, *Nature*, 2007, **450**, 1001–1009.
5 D. A. Giljohann, D. S. Seferos, W. L. Daniel, M. D. Massich, P. C. Patel and C. A. Mirkin, *Angew. Chem., Int. Ed.*, 2010, **49**, 3280–3294.
6 K. Saha, S. S. Agasti, C. Kim, X. N. Li and V. M. Rotello, *Chem. Rev.*, 2012, **112**, 2739–2779.
7 For representative examples, see: (*a*) J. P. Tam, *Proc. Natl. Acad. Sci. U. S. A.*, 1988, **85**, 5409–5413; (*b*) G. A. Kinberger, W. B. Cai and M. Goodman, *J. Am. Chem. Soc.*, 2002, **124**(51), 15162–15163; (*c*) A. Esposito, E. Delort, D. Lagnoux, F. Djojo and J. L. Reymond, *Angew. Chem., Int. Ed.*, 2003, **42**, 1381–1383; (*d*) T. Darbre and J. L. Reymond, *Acc. Chem. Res.*, 2006, **39**, 925–934.
8 For representative examples, see: (*a*) R. Levy, N. T. K. Thanh, R. C. Doty, I. Hussain, R. J. Nichols, D. J. Schiffrin, M. Brust and D. G. Fernig, *J. Am. Chem. Soc.*, 2004, **126**, 10076–10084; (*b*) F. Maran, L. Fabris, S. Antonello, L. Armelao, R. L. Donkers, F. Polo and C. Toniolo, *J. Am. Chem. Soc.*, 2006, **128**, 326–336; (*c*) C. C. You, S. S. Agasti and V. M. Rotello, *Chem. – Eur. J.*, 2008, **14**, 143–150; (*d*) L. Maus, O. Dick, H. Bading, J. P. Spatz and R. Fiammengo, *ACS Nano*, 2010, **4**, 6617–6628; (*e*) I. M. Rio-Echevarria, R. Tavano, V. Causin, E. Papini, F. Mancin and A. Moretto, *J. Am. Chem. Soc.*, 2011, **133**, 8–11.
9 For representative examples, see: (*a*) M. R. Ghadiri, J. R. Granja, R. A. Milligan, D. E. McRee and N. Khazanovich, *Nature*, 1993, **366**, 324–327; (*b*) M. Reches and E. Gazit, *Science*, 2003, **300**, 625–627; (*c*) A. M. Smith, R. J. Williams, C. Tang, P. Coppo, R. F. Collins,

M. L. Turner, A. Saiani and R. V. Ulijn, *Adv. Mater.*, 2008, **20**, 37–41; (*d*) B. Rubinov, N. Wagner, H. Rapaport and G. Ashkenasy, *Angew. Chem., Int. Ed.*, 2009, **48**, 6683–6686.
10 L. J. Prins, *Acc. Chem. Res.*, 2015, **48**, 1920–1928.
11 (*a*) F. Della Sala and E. R. Kay, *Angew. Chem., Int. Ed.*, 2015, **54**, 4187–4191; (*b*) S. Borsley and E. R. Kay, *Chem. Commun.*, 2016, DOI: 10.1039/C6CC00135A.
12 (*a*) P. Nowak, V. Saggiomo, F. Salehian, M. Colomb-Delsuc, Y. Han and S. Otto, *Angew. Chem., Int. Ed.*, 2015, **54**, 4192–4197; (*b*) Y. Han, P. Nowak, M. Colomb-Delsuc, M. P. Leal and S. Otto, *Langmuir*, 2015, **31**, 12658–12663.
13 S. Maiti and L. J. Prins, *Chem. Commun.*, 2015, **51**, 5714–5716.
14 M. J. Hostetler, J. E. Wingate, C. J. Zhong, J. E. Harris, R. W. Vachet, M. R. Clark, J. D. Londono, S. J. Green, J. J. Stokes, G. D. Wignall, G. L. Glish, M. D. Porter, N. D. Evans and R. W. Murray, *Langmuir*, 1998, **14**, 17–30.
15 (*a*) A. V. Ellis, K. Vjayamohanan, R. Goswaimi, N. Chakrapani, L. S. Ramanathan, P. M. Aiayan and G. Ramanath, *Nano Lett.*, 2003, **3**, 279–282; (*b*) R. L. Phillips, O. R. Miranda, D. E. Mortenson, C. Subramani, V. M. Rotello and U. H. F. Bunz, *Soft Matter*, 2009, **5**, 607–612; (*c*) B. Perrone, S. Springhetti, F. Ramadori, F. Rastrelli and F. Mancin, *J. Am. Chem. Soc.*, 2013, **135**, 11768–11771; (*d*) G. Pieters, C. Pezzato and L. J. Prins, *Langmuir*, 2013, **29**, 7180–7185.
16 S. Maiti, C. Pezzato, S. Garcia Martin and L. J. Prins, *J. Am. Chem. Soc.*, 2014, **136**, 11288–11291.
17 C. Franceschini, P. Scrimin and L. J. Prins, *Langmuir*, 2014, **30**, 13831–13836.

